Journal of Hydrology 561 (2018) 312–321

Contents lists available at ScienceDirect

Journal of Hydrology

journal homepage: www.elsevier.com/locate/jhydrol

Research papers

Runoff sensitivity to climate change in the Nile River Basin

Emad Hasan[a,b,e,*], Aondover Tarhule[a,b], Pierre-Emmanuel Kirstetter[b,c], Race Clark III[d], Yang Hong[b,c]

[a] Department of Geography, State University of New York, SUNY at Binghamton, NY, USA
[b] Hydrometrology and Remote Sensing (HyDROS) Laboratory, Advanced Radar Research Center (ARRC), University of Oklahoma, Norman, OK, USA
[c] School of Civil Engineering and Environmental Sciences, University of Oklahoma, Norman, OK, USA
[d] Cooperative Institute for Mesoscale Meteorological Studies, University of Oklahoma, Norman, OK, USA
[e] Geology Department, Faculty of Science, Damietta University, New Damietta, Egypt

ARTICLE INFO

This manuscript was handled by Emmanouil Anagnostou, Editor-in-Chief

Keywords:
Climate change
Nile River Basin
Runoff elasticity
Water resources

ABSTRACT

In data scarce basins, such as the Nile River Basin (NRB) in Africa, constraints related to data availability, quality, and access often complicate attempts to estimate runoff sensitivity using conventional methods. In this paper, we show that by integrating the concept of the aridity index (AI) (derived from the Budyko curve) and climate elasticity, we can obtain the first order response of the runoff sensitivity using minimal data input and modeling expertise or experience. The concept of runoff elasticity relies on the fact that the energy available for evapotranspiration plays a major role in determining whether the precipitation received within a drainage basin generates runoff. The approach does not account for human impacts on runoff modification and or diversions. By making use of freely available gauge-corrected satellite data for precipitation, temperature, runoff, and potential evapotranspiration, we derived the sensitivity indicator (β) to determine the runoff response to changes in precipitation and temperature for four climatic zones in the NRB, namely, tropical, subtropical, semiarid and arid zones. The proposed sensitivity indicator can be partitioned into different elasticity components i.e: precipitation (ε_p), potential evapotranspiration (ε_{ETp}), temperature (ε_T) and the total elasticity (ε_{tot}). These elasticities allow robust quantification of the runoff response to the potential changes in precipitation and temperature with a high degree of accuracy. Results indicate that the tropical zone is energy-constrained with low sensitivity, ($\beta < 1.0$), implying that input precipitation exceeds the amounts that can be evaporated given the available energy. The subtropical zone is subdivided into two distinct regions, the lowland (Machar and Sudd marshes), and the highland area (Blue Nile Basin), where each area has a unique sensitivity. The lowland area has high sensitivity, ($\beta > 1.0$). The subtropical-highland zone moves between energy-limited to water-limited conditions during periods of wet and dry spells with varying sensitivity. The semiarid and arid zones are water limited, with high sensitivity, ($\beta > 1.0$). The calculated runoff elasticities show that a 10% decrease in precipitation leads to a decrease in runoff of between 19% in the tropical zone and 30% in the arid zones. On the other hand, a 10% precipitation increase leads to a runoff increase of 14% in the tropical zone and 22% in the arid zone. The estimated runoff changes are consistent with the result obtained using other methods. Thus, the elasticity approach combines data parsimony and analytical simplicity to produce results that are practically useful for most purposes while facilitating communication with stakeholders with different levels of scientific knowledge. More research is needed to extend the application of the method to incorporate the effects of human activities, and land use change.

1. Introduction

The Nile River Basin (NRB) is characterized by extreme hydroclimatic variability over space and time (Conway, 2005; Camberlin, 2009; Elshamy et al., 2009a; UNEP, 2013), complicated hydro-politics governed by numerous agreements and pacts (Swain, 2011; Martens, 2011; Ibrahim, 2011), and rapid population and environmental changes (Mohamed and Loulseged, 2008; Williams, 2009). Climate change will almost certainly complicate these dynamics. For example, Labat et al. (2004) calculated that a 1 °C mean annual temperature increase would negatively impact runoff response throughout Africa's major river basins. In the Nile Basin, specifically, mean annual temperature is

* Corresponding author at: Department of Geography, The State University of New York, SUNY at Binghamton, Binghamton, NY 13902, USA.
E-mail address: emad.hasan@binghamton.edu (E. Hasan).

https://doi.org/10.1016/j.jhydrol.2018.04.004
Received 30 November 2017; Received in revised form 10 February 2018; Accepted 1 April 2018
Available online 03 April 2018
0022-1694/ © 2018 Elsevier B.V. All rights reserved.

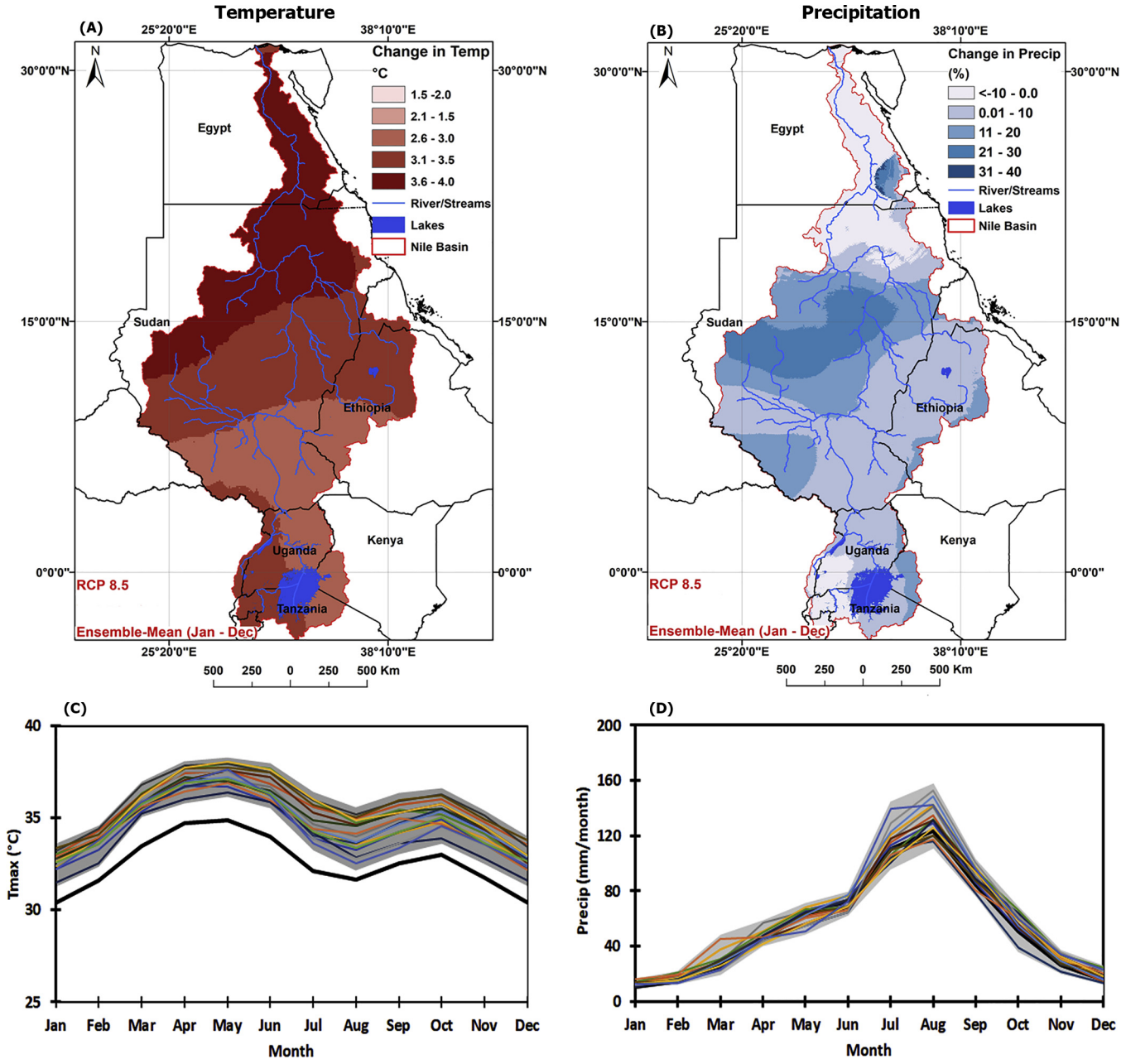

Fig. 1. Future changes in temperature (A) and precipitation (B) across NRB for the year 2050 using ensemble mean of 17 GCMs for RCP 8.5 emission scenario, changes calculated relative to baseline (1960–1990). Mean annual temperature is expected to rise (C) relative to baseline (thick black line), while GCMs disagree on the direction of precipitation change (D).

expected to rise by between 2.0 °C and 4.0 °C (± 0.28 °C) by mid-century (Fig. 1; (IPCC, 2014; Fick and Hijmans, 2017)). With respect to precipitation (P), climate models disagree on the direction of future precipitation change (Elshamy et al., 2009b), with estimates ranging from −12% to +24%. The combination of above changes may alter existing tenuous systems for managing the hydroclimatic variability within the basin and disrupt best practices based on history and current knowledge. Such risk has prompted numerous modeling efforts with varying degrees of complexity to predict how different sectors are likely to respond to diverse types of perturbations and human activities (Beyene et al., 2009; Elshamy et al., 2009a; Oestigaard, 2010; Setegn et al., 2011; Taye et al., 2011; NIS, 2012; Dile et al., 2013; Dessie et al., 2014; Hasan et al., 2015).

Ideally, basin-scale hydrologic models offer the most comprehensive and reliable means of capturing the hydroclimatic response to changes within a basin (Gudmundsson et al., 2012). In practice, however, the outputs of any modeling exercise are only as good as the completeness, quality, and spatiotemporal representativeness of available input data. Where the necessary data are lacking, as is the case in the NRB, even the most sophisticated models often produce equivocal results that are difficult to interpret and may not justify the expense of efforts and resources.

As an alternative, sensitivity analysis or elasticity of one variable (e.g. runoff, R) to concurrent changes in other variables (e.g. precipitation and temperature) have been shown to produce results useful for many applications. The runoff elasticity to precipitation change, ε_p, is defined as the proportional change in mean annual runoff divided by the proportional change in mean annual precipitation (Schaake, 1990; Chiew et al., 2006). In other words, ε_p is a measure of the degree to which runoff is sensitive, or responds, to changes in precipitation, *under*

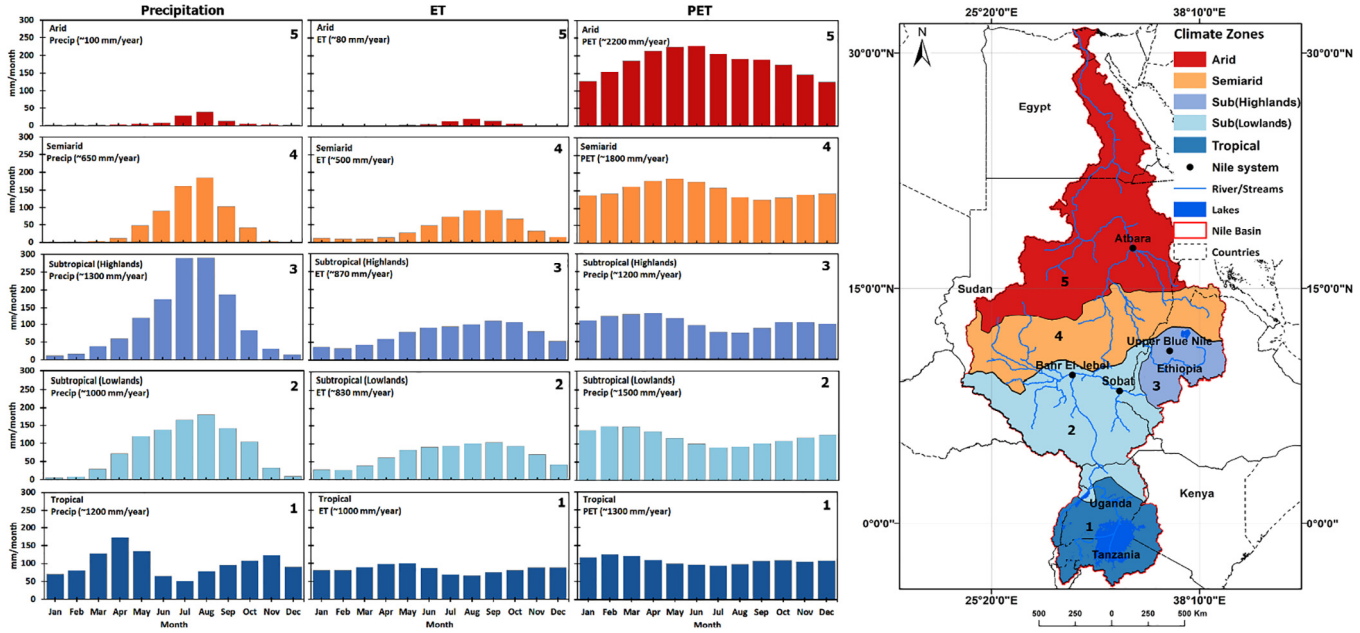

Fig. 2. Monthly average precipitation, ET_a, and ET_p (1960 to 2015) across the four main climate zones; the tropical, subtropical, semiarid and arid climate zones. The four main tributaries: Bahr El-Jabel, Sobat, Upper Blue Nile and Atbara, are shown on the map.

natural conditions. Low values of ε_p imply that relatively large changes in precipitation produce relatively small responses in surface runoff. Conversely, large values of ε_p imply that relatively small changes in precipitation produce relatively large responses in surface runoff. For instance, an elasticity of 2.0 indicates that a 1.0% change in precipitation results in a 2.0% change in streamflow, while a 10% change in precipitation results in a 20% change in the runoff.

A major advantage of the sensitivity or elasticity approach is the parsimony of data requirement. For example, to estimate ε_p, one requires only observations on the *Q-P-T* relationship, as well as expected future change in *P-T*. Furthermore, the method can be implemented even with limited or no modeling experience. Finally, the results are in a form that is easily understood by stakeholders with different levels of scientific knowledge [see Schaake (1990)], making it a useful communication tool. On the other hand, this simplification comes at a cost. As a general rule, significant natural changes such as extreme hydroclimatic variability, or anthropogenic activities, such as land use modification or surface water diversion and storage which alter the runoff-precipitation-temperature relationship, also affect the ε_p estimates. This limitation is not unique to this method and implies that estimates of ε_p need to be updated periodically to account for the dynamic nature of the runoff-precipitation-temperature relationship.

Even so, the method has been shown to produce results that are of an order of accuracy comparable to many models and sufficient for most practical applications (Dooge et al., 1999; Sankarasubramanian et al., 2001; Chiew, 2006; Chiew et al., 2006; Harman et al., 2011; Yang and Yang, 2011). For example, in the Blue Nile Basin (BNB), Conway and Hulme (1996) showed that a 10% precipitation increase would yield 25–30% change in surface runoff (Conway and Hulme, 1996). Similarly, in the Niger River Basin of West Africa, Grijsen et al. (2013), calculated the runoff elasticity to be about 2.5, meaning that a 10% change in precipitation produces a 25% change in runoff, consistent with the results obtained using MIKE HYDRO Basin water resources allocation model for the Niger Basin.

In this study, we estimate the runoff elasticity for the entire NRB as well as for each bio-climatic zone within the basin using a newly introduced sensitivity indicator (β). This research contributes to expanding the range of applications of the global hydrological datasets to study the hydrology of a complex basin such as the Nile. Using gauge-corrected grids, especially where *in-situ* data are inaccessible can help to address major hydrological challenges and better manage the water resources. The study approach also represents a simple but rapid, efficient and reliable methodology for estimating basin-wide sensitivity using a single indicator, β, that can be derived using minimal data input. Notably, β can be easily partitioned into different elasticities, including elasticity to precipitation, temperature and potential evapotranspiration, to understand the runoff responses. The results are intuitive to understand and easy to communicate with stakeholders. The results also add to the growing literature on efforts to examine how changes in temperature and precipitation could affect runoff and thus the water balance over the NRB and other data scarce regions. The rest of the paper is organized as follows: Section 2 briefly describes the study area and outlines datasets and methods; Section 3 contains results and discussion, and Section 4 is a summary of major findings.

2. Data and methods

2.1. Study area

With total flow length of over 6700 km, the Nile is the world's longest river. Its drainage basin covers approximately 1.3 million km^2, equivalent to 10% of Africa's landmass. More than 400 million people inhabit the basin (2012 estimate), distributed among 11 countries (Burundi, Democratic Republic of Congo, Egypt, Eritrea, Ethiopia, Kenya, Rwanda, South Sudan, Sudan, Tanzania, and Uganda). The basin's population is projected to increase to 700 million by the year 2030, raising concerns about sustainability and equitable management of the basin's resources (Abtew and Melesse, 2014). Physically, the NRB encompasses five climate zones namely, tropical, subtropical, semiarid, arid and Mediterranean (Shahin, 1985), each possessing a distinctive pattern of precipitation, temperature, and evapotranspiration (Fig. 2). The seasonal precipitation distribution is bimodal in the tropical zone, with mean annual approximately 1200 mm over the period 1960–2015. Precipitation distribution is unimodal in the subtropical zone, concentrated in the months from May to October, with mean seasonal approximately 1100 mm over the same period. In the semiarid and arid zones, mean annual precipitation averages, respectively 650 mm and 100 mm, concentrated between November to March (Fig. 2). A portion

of the Nile Delta in the extreme northern limits of the basin experiences a Mediterranean climate regime with rainfall average of 200–100 mm/year (Camberlin, 2009; UNEP, 2013).

The spatial pattern of the mean annual actual evapotranspiration (ET_a) is similar to the precipitation pattern, being higher in the tropical and subtropical zones and declining toward the semiarid and arid zones. For instance, the tropical zone has mean seasonal total ET_a of approximately 1000 mm over the period 1960–2015, while the arid zone has a mean seasonal average of 80 mm over the same period. The potential evapotranspiration (ET_p) grades in the opposite direction, being relatively low in tropical and subtropical zones, while high in the semiarid and arid zones (Camberlin, 2009). The topical area has mean annual ET_p of 1300 mm/year, while in the arid zone, ET_p exceeds 2000 mm/year.

The Runoff distribution reflects the spatial and temporal patterns of precipitation. Three main river systems drain runoff in the Nile basin, namely the White Nile (including the Bahr El-Jabel and Sobat), Upper Blue Nile and Atbara. The White Nile, measured at its confluence with the Bahr El-Jabel and Sobat, generates approximately 24% of total runoff and the Upper Blue Nile contributes about 60% of the total flow. The Atbara accounts for the remaining 16% of the basin runoff. The arid zone contributes almost no runoff to the Nile's flow.

2.2. Datasets

Given the limited availability and access to *in-situ* observations over the NRB, this study utilized freely available gauge-corrected satellite data for precipitation, temperature, runoff, ET_a and ET_p. Table 1 summarizes the types, sources and spatial resolutions of the data used in the study. Despite the recent advances in satellite observations, blended and reanalysis grids, our understanding of the hydrology of complex data-poor basins remains limited. The gauge-corrected grids provide valuable hydrological data that fills gaps in *in-situ* observations over space and time. Global hydrological data sets are critical sources of information for assessing water resources at various spatial and temporal scales. In this study, the monthly gauge-corrected precipitation data were obtained from the Global Precipitation Climate Center (GPCC; version 5) (Schneider et al., 2011) (http://gpcc.dwd.de) for the period from 1960 to 2015 at 0.5°. The monthly reanalysis temperature, and ET_p (version CRU TS 3.24.01) data were obtained from the Climate Research Unit (CRU) at the University of East Anglia. The CRU dataset is based on more than 4000 weather stations around the world and has spatial resolution of 0.5° × 0.5° for all variables (Jones and Harris, 2013). The data are archived at http://www.cru.uea.ac.uk/data and include several climate variables (e.g. precipitation, air temperature, ET_p, the Palmer Drought Severity Index [PDSI], and the wet-day frequency), dating back to 1901. The ET_a grids were derived according to a method introduced by Zhang et al. (2010) and archived at the Hydrometrology and Remote Sensing (HyDROS) Laboratory, University of Oklahoma (http://hydro.ou.edu/research/data/). Finally, the surface runoff estimates are mean annual merged gauge runoff data acquired from the Global Runoff Data Center (GRDC) at 0.5° resolution and available at http://www.bafg.de/GRDC/ (Fekete et al., 2002).

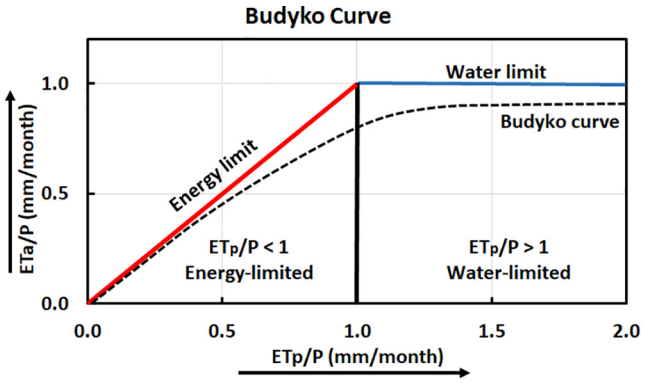

Fig. 3. Illustration of the Budyko Curve.

2.3. Conceptual framework

The concept of runoff elasticity relies on the fact that the energy available for evapotranspiration plays a major role in determining whether the precipitation received within a drainage basin generates runoff (Creed et al., 2014). The concept builds upon the work of Budyko (1974) who developed two indices, i.e. the evaporative index (*EI*) and the aridity index (*AI*) defined as:

$$EI = \frac{ET_a}{P}, \tag{1}$$

$$AI = \frac{ET_p}{P}, \tag{2}$$

where P is precipitation, and ET_a, ET_p are as defined previously.

When ET_p<P (i.e. $AI < 1.0$), the basin generates runoff because available energy is insufficient for evaporating all incident precipitation, and the basin is described as energy limited. Conversely, when ET_p>P (i.e. $AI > 1.0$), the energy available for evapotranspiration exceeds available precipitation (water becomes a limiting factor) and the basin produces no runoff (Fig. 3). Budyko's Curve shows the expected runoff response for any basin based on the relationships among P, ET_a and ET_p. These relationships have been utilized in various studies as a reference for the water balance condition in a basin or catchment (Arora, 2002; Di Baldassarre et al., 2011; Creed et al., 2014; van der Velde et al., 2014).

According to Arora (2002), the change in surface runoff (ΔQ) can be expressed as a function of the change in precipitation (ΔP) minus ΔET_p, the change in *ETp* :

$$\frac{\Delta Q}{Q} = \frac{\Delta P}{P}(1+\beta) - \frac{\Delta ET_p}{ET_p}\beta \tag{3}$$

where the coefficient β is the sensitivity index, the value of which is proportional to the aridity index (Arora, 2002). Generally, β is estimated for a given climate zone by calculating the runoff coefficient, Rc, using the evaporative index as:

$$Rc = \frac{Q}{P} = 1 - \frac{ET_a}{P} = 1 - EI \tag{4}$$

Following Grijsen et al. (2013), the coefficient β can be estimated

Table 1
Summary of the types, sources and spatial resolutions of the data used in the study.

Data type	Data source	Resolution	Reference	Description
Precipitation	GPCC, http://gpcc.dwd.de	0.5°	Schneider et al. (2011)	Gauge-corrected
Temperature	CRU, http://www.cru.uea.ac.uk/data	0.5°	Jones and Harris (2013)	Reanalysis data
Potential ET	CRU, http://www.cru.uea.ac.uk/data	0.5°	Jones and Harris (2013)	Reanalysis data
Actual ET	http://hydro.ou.edu/research/data/	0.5°	Zhang et al. (2010)	Reanalysis data
Runoff	GRDC, http://www.bafg.de/GRDC/	0.5°	Fekete et al. (2002)	Gauge-corrected

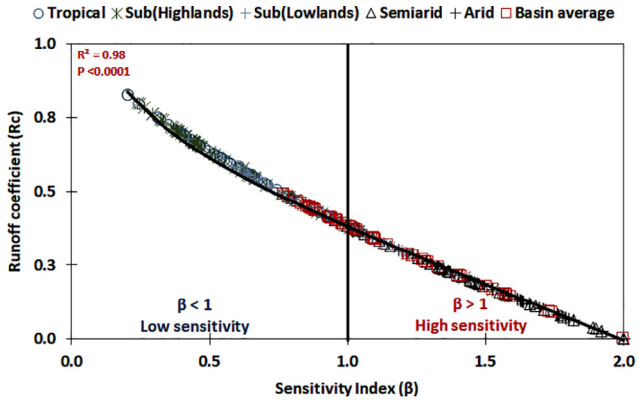

Fig. 4. The sensitivity index (β) is inversely proportional to the runoff coefficient (Rc); as sensitivity increases the runoff coefficient decreases substantially.

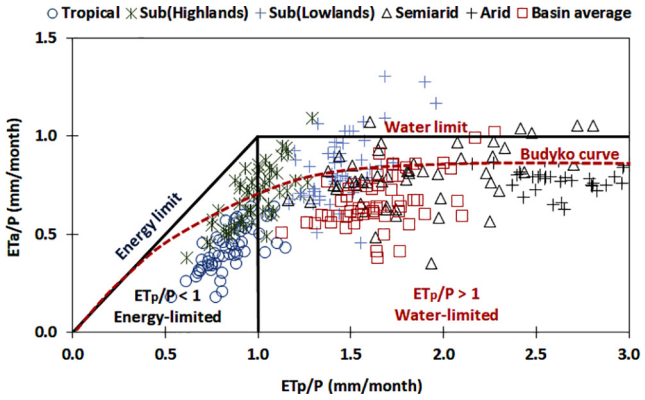

Fig. 6. Relationship between ET_p and ET_a, each normalized by precipitation, for presentation in Budyko space (data from 1960 to 2015). On average, the NRB is water-limited due to the distribution of these climate zones.

as:

$$\beta = 2-3 \times (Rc) + (Rc)^2 \quad (5)$$

When β is large, a given change in either precipitation or ET_p produces disproportionate changes in surface runoff. Further, β is largest at the point where Rc is lowest (see, Fig. 4).

From Eq. (3), ε_p, the surface runoff elasticity to precipitation, can be expressed as follows:

$$\varepsilon_p = \frac{[\frac{\Delta Q}{Q}]}{[\frac{\Delta P}{P}]} = 1 + \beta \quad (6)$$

Similarly, ε_{ET_p}, the surface runoff elasticity to ET_p, can be expressed as:

$$\varepsilon_{ET_p} = \frac{[\frac{\Delta Q}{Q}]}{[\frac{\Delta ET_p}{ET_p}]} = -\beta \quad (7)$$

And ε_T, the surface runoff elasticity to temperature can be calculated according to Grijsen et al. (2013) as:

$$\varepsilon_T = \frac{[\frac{\Delta Q}{Q}]}{[\frac{\Delta T}{T}]} = \varepsilon_{ET_p} \times T/(T + 17.8) = -0.60 \times \beta \quad (8)$$

Finally, the total elasticity, ε_{tot}, can be determined as

$$\varepsilon_{tot} = 1 + \beta - 0.60 \times \beta \quad (9)$$

For simplicity, ε_{ET_p}, ε_T, and ε_{tot} can be expressed as functions of the ε_p as following:

Table 2
Summary of average runoff elasticity to various quantities for each climate zone in the NRB. The results are based on data from 1960 to 2015, the elasticities are calculated for the extreme periods (dry and wet).

Region		Period	β	ε_p	ε_{ETp}	ε_T	ε_{tot}
Tropical		Dry	0.90	1.90	−0.90	−0.54	0.46
		Wet	0.45	1.45	−0.45	−0.27	0.73
		Aver.	0.59	1.59	−0.59	−0.35	0.65
Subtropical	Lowlands	Dry	1.70	2.70	−1.70	−1.02	0.58
		Wet	1.01	2.01	−1.01	−0.61	0.99
		Aver.	1.26	2.26	−1.26	−0.77	0.84
	Highlands	Dry	1.38	2.38	−1.38	−0.83	0.77
		Wet	0.98	1.98	−0.98	−0.58	1.01
		Aver.	1.06	2.06	−1.06	−0.64	0.96
Semiarid		Dry	1.80	2.80	−1.80	−1.08	−0.08
		Wet	1.02	2.02	−1.02	−0.61	0.39
		Aver.	1.46	2.46	−1.46	−0.88	0.12
Arid		Dry	1.98	2.98	−1.98	−1.19	−0.19
		Wet	1.28	2.28	−1.28	−0.77	0.23
		Aver.	1.65	2.65	−1.65	−0.99	0.01
Basin Average		Dry	1.50	2.5	−1.5	−0.90	0.10
		Wet	0.95	1.95	−0.95	−0.57	0.43
		Aver.	1.14	2.14	−1.14	−0.68	0.32

$$\varepsilon_{ET_p} = -\varepsilon_p + 1 \quad (10)$$

$$\varepsilon_T = -0.6 \times \varepsilon_p + 0.6 \quad (11)$$

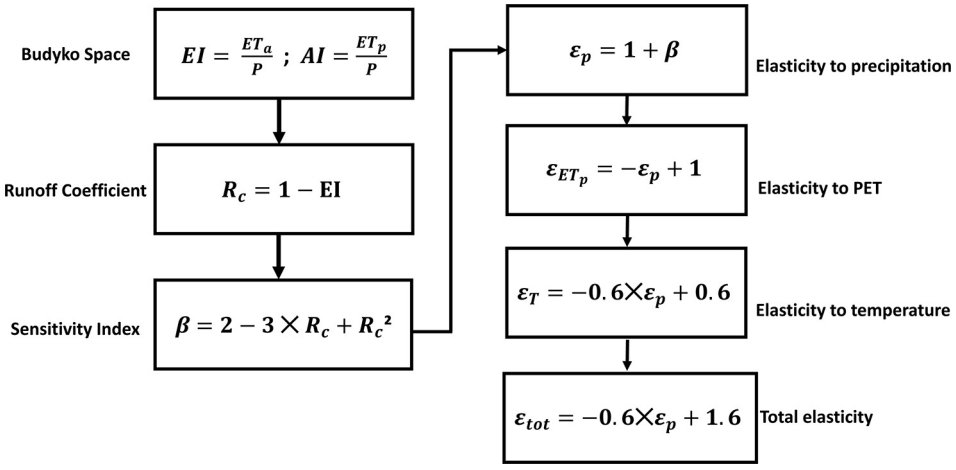
Budyko Space
EI = ET_a / P ; AI = ET_p / P
Runoff Coefficient
R_c = 1 − EI
Sensitivity Index
β = 2 − 3 × R_c + R_c²
ε_p = 1 + β
Elasticity to precipitation
ε_ETp = −ε_p + 1
Elasticity to PET
ε_T = −0.6×ε_p + 0.6
Elasticity to temperature
ε_tot = −0.6×ε_p + 1.6
Total elasticity

Fig. 5. Schematic framework for calculating ε_p, ε_{ET_p}, and ε_T.

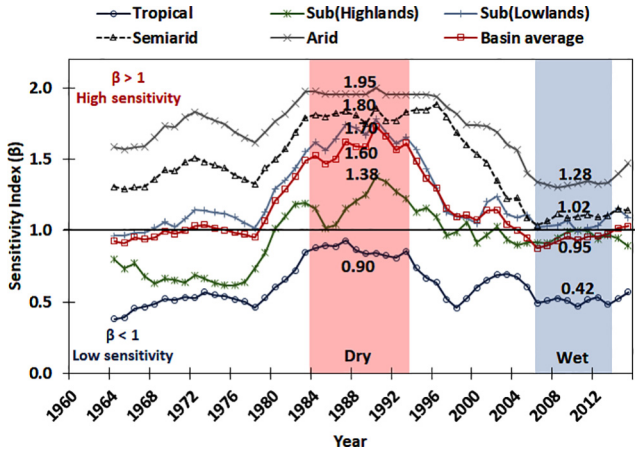

Fig. 7. The β indicator, normalized using five-year moving average, from 1960 to 2015 to reflect the general sensitivity of each climate zone during stress (extreme dry) as highlighted in red and recovery (extreme wet) conditions as highlighted in blue. The overall average is shown in the figure. (For interpretation of the references to colour in this figure legend, the reader is referred to the web version of this article.)

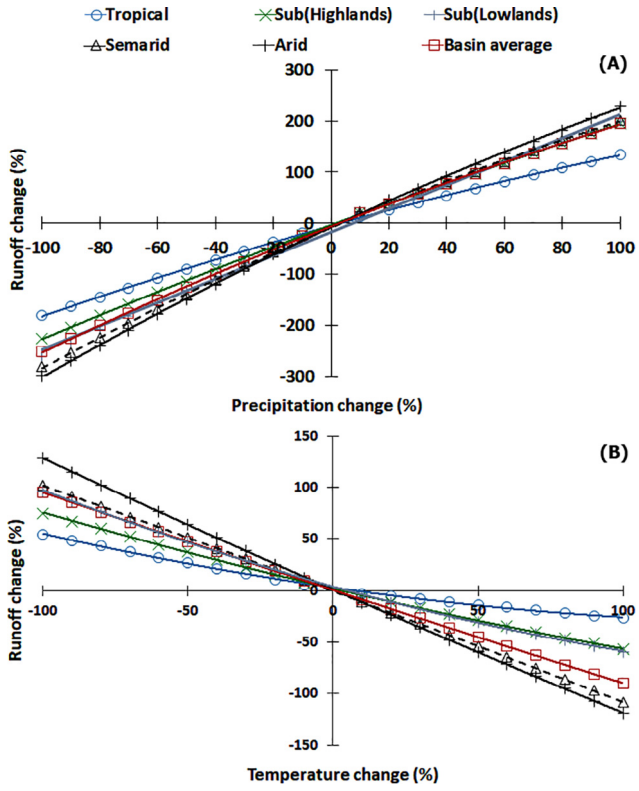

Fig. 8. The relative change in a runoff to precipitation (A) and temperature (B) changes.

$$\varepsilon_{tot} = -0.6 \times \varepsilon_p + 1.6 \tag{12}$$

The above concepts were utilized to assess the sensitivity of runoff in the NRB to projected climate change. As we noted above, β can be mathematically partitioned into different elasticity components (i.e. precipitation, temperature and potential ET). Thus, once the sensitivity indicator is determined, we can derive different elasticity values. Fig. 5 schematically illustrates the analytic framework. First, we developed the Budyko Curve for the basin, from which we calculated the aridity and evaporative indices. Second, the change rate under the Budyko space (the coefficient β) was determined from Eq. (5), which was then used to calculate ε_p, ε_{ET_p}, and ε_T. Third, Eq. (9) was developed to calculate ε_{tot}.

3. Results and discussion

3.1. Budyko curve analysis

Fig. 6 shows the Budyko Curve for the NRB based on data from 1960 to 2015. Consistent with the basin's known physical and climatological dynamics, the tropical and subtropical (highlands) areas map generally into the energy-limited conditions. During periods of anomalously extreme dry spells, the highland region becomes water constrained and maps under the water-limited region in the Budyko space. The subtropical lowlands are considered water limited zones with high evapotranspiration potentials. The lowland zone receives significant amounts of surface water and possesses expansive swamps and marshes (i.e. the *Sudd*), represented by the data points that plot above the water limits. Both the semiarid and arid zones map into the water-limited space but for entirely different reasons. The semiarid zone, characterized by high rates of evapotranspiration, loses substantial quantities of water to the atmosphere. The arid zone is absolutely a water-limited zone due to both limited water input (low precipitation) and high temperatures, which act to increase ET_p. On average, the NRB as a whole is water-limited, because more than half its area falls into semiarid or arid zones with limited water yields. It can be concluded that in the absence of any change in ET_p, surface runoff amounts are largely driven by changes in precipitation. Conversely, in the absence of changes in precipitation, the variation in surface runoff is mainly governed by ΔET_p, as in the semiarid and arid zones.

According to Eq. (9), the ε_{tot}, reflects the combined effects of the changes in precipitation, potential ET and temperature on surface runoff. Generally, $\varepsilon_{tot} > 0.5$ during wet periods, and $\varepsilon_{tot} < 0.5$ during dry periods. As total elasticity increases runoff generation also increases. The zones with ε_{tot} close to or greater than 1.0 are prominent water source areas. Table 2 shows the illustrative elasticity estimates across the NRB during two periods of extreme conditions. Section 3.2 below explores these dynamics in greater detail.

3.2. Sensitivity and elasticity analysis

As explained previously, the sensitivity index β is inversely proportional to the surface runoff coefficient Rc (see Fig. 4). Thus, the tropical zone is characterized by low sensitivity ($\beta < 1.0$) and high runoff potential ($Rc > 0.40$). The subtropical-lowland zone is highly sensitive zone ($\beta > 1.0$), while the subtropical-highland area fluctuates between the water and energy limits with varying sensitivities. The semiarid and arid zones are very sensitive ($\beta > 1.0$) and show very low runoff ($Rc < 0.10$). It is worth noting that β changes over time; it is lower during wet periods and higher during dry spells, similar to its change spatially from areas of water surfeit, such as the tropics, to the water deficit arid zone (Fig. 7). Similarly, β also changes periodically in response drought and wet regimes across the basin.

Based on the β indicator, the runoff elasticities ε_p, ε_{ET_p}, ε_T and ε_{tot} were calculated as shown in Eqs. (6), (10), (11), and (12). To understand the implications of these calculations, Table 2 summaries the average elasticities, as well as the elasticities during extreme conditions, for each climate zone and the entire basin. For instance, the elasticity analysis shows an average ε_p of 1.59, 2.26, 2.06, 2.46 and 2.65 respectively for the tropical, subtropical-lowland, subtropical-highlands, semiarid and arid zones. The calculated ε_p was used to determine the runoff changes by rearranging Eq. (7) as follows:

$$\frac{\Delta Q}{Q} = \varepsilon_p \times \frac{\Delta P}{P} \tag{13}$$

Using the above relation, the relative change in runoff to the precipitation change can be obtained, as shown in Fig. 8A. According to

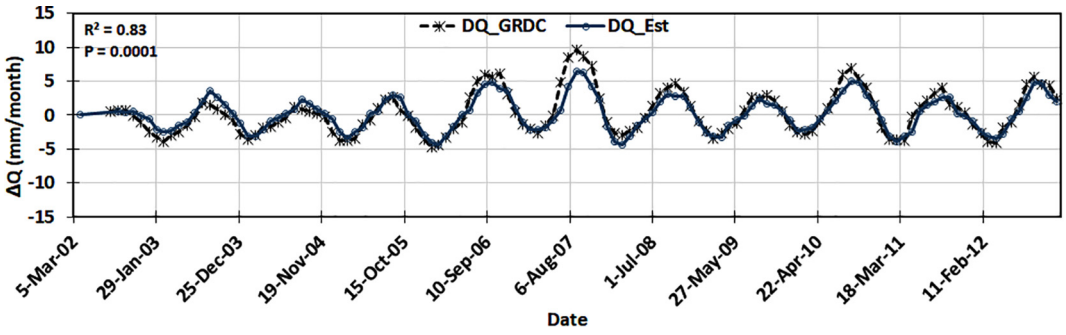

Fig. 9. Basin average estimated runoff changes using the relationship between rainfall changes $\Delta P/P$, and ε_p, compared to the estimated runoff changes (DQ_Est) using the gauge corrected GRDC (DQ_GRDC) runoff grids from (2002 to 2012).

Table 3
The changes in the surface runoff under current and future precipitation and temperature changes for the NRB, broken down by climate zone, future changes in runoff were calculated using the extreme ends of precipitation and temperature changes.

Region		Runoff changes (1960–2015)				Runoff changes (2050) (RCP 8.5)			
		P (± 10%)		*T*(± 1.0°)		*P*		*T*(± 2.0°)	
		Dry	Wet	Dry	Wet	Dry (−12%)	Wet (+24%)	Dry	Wet
Tropical		−19.0	14.5	−0.54	0.27	−22.8	34.8	−1.08	0.54
Subtropical	Lowlands	−27.0	20.0	−1.02	0.61	−32.4	48.2	−2.04	1.22
	Highlands	−24.0	19.8	−0.83	0.58	−28.8	47.5	−1.66	1.16
Semiarid		−28.0	20.0	−1.08	0.61	−33.6	48.0	−2.16	1.22
Arid		−30.0	23.0	−1.19	0.77	−35.8	54.07	−2.38	1.54
Basin average		−25.0	19.5	−0.90	0.57	−30.0	46.8	−1.80	1.14

this relation, a 10% precipitation increase leads to a runoff increase of 12% in the tropical zone and 18% in the arid zone. On the other hand, a 10% precipitation decrease results in a 10% runoff loss in the tropical region and 28% in the arid zone. Similarly, we can estimate relative changes in runoff to ET_p and temperature, as well as their combined effects (ε_{tot}) by rearranging each corresponding equation (Table 2).

As an example of a practical application, we use Eq. (4) to produce runoff estimates over the basin. The resulting runoff change is computed and compared with the runoff changes using the available gauge corrected runoff grids of the Global Runoff Data Center (GRDC) runoff data from 2002 to 2012 (Fig. 9). The simulated runoff explains over 80% ($R^2 = 0.83$) of the variation in the observed runoff. In the same way, future changes can be assessed using the calculated elasticity values and projected precipitation and temperature changes. For example, utilizing the extreme ends of GCM projected changes in precipitation and temperature, Table 3 provides the corresponding runoff change (%) for each climate zone and the entire Nile Basin for 2050. Similar runoff estimates can be obtained readily for any desired level of precipitation and temperature changes.

The estimated runoff changes in Table 3 compare favorably with those obtained using other methods. For example, based on the analysis of precipitation and temperature records in BNB, Conway (2005) estimated that a 10% increase in precipitation will lead to 30% increase in runoff. Similarly, using analysis of the GCMs, Siam, and Eltahir (2017) projected a 15% increase in the runoff over the BNB by 2050 (Siam and Eltahir, 2017). Over the entire Nile Basin, Schaake (1990) and Chiew et al. (2006) independently obtained a runoff elasticity of 2.5, corresponding to an expected 25% runoff increase. It is important to note that due to non-linearity in the runoff-precipitation-temperature relationship, negative changes of comparable magnitude do not always produce similar responses. That is, −10% decline in precipitation does not automatically imply a 25% reduction in runoff. Studies of runoff sensitivity analysis have also been carried out at basin scale for several major African river systems, including Blue Nile Basin (BNB), Niger, Congo, and Okavango river basins (Gleick, 1991; Chiew et al., 2006; Elshamy et al., 2009b; Hasan and Elshamy, 2011; Gebrekristos, 2015).

Hence, despite the analytical simplicity and parsimonious parameters, the elasticity approach produces future runoff estimates comparable to those obtained from more computationally intensive and data demanding modeling methods. We posit, therefore, that the elasticity approach can be used as a first estimate or in applications where high-level accuracy is neither necessary nor feasible, to produce practically useful results and to identify the scope for furthermore complex analysis.

Fig. 10 presents the results of the estimated runoff changes according to the calculated elasticities of ε_p, and ε_T for current and future precipitation and temperature over the NRB. Clearly, the estimated runoff changes are driven by projected precipitation and temperature changes (see Fig. 1). Further, the spatial patterns of the runoff response to precipitation and temperature are consistent with the distribution of regions of water and energy limits. We recognize that in practice, precipitation, temperature and evapotranspiration changes interact in complex ways that may result in runoff changes that are different from the arithmetic sum of the expected response to each individual variable taken separately. We argue that while legitimate theoretically, inadequate data and knowledge of the physical dynamical relationship among P, T, ET_p and Q frequently lead to results that are not necessarily better than those obtained with the simplified assumptions of the elasticity method.

4. Summary and conclusions

Runoff is critically important in many human, ecological and economic activities, hence, ability to estimate possible runoff change in response to changes in precipitation and temperature is highly desirable. Complicating this task, however, are constraints related to data access or lack of data at the density, quality and the desired level of completeness. The NRB exemplifies these conditions. The results of

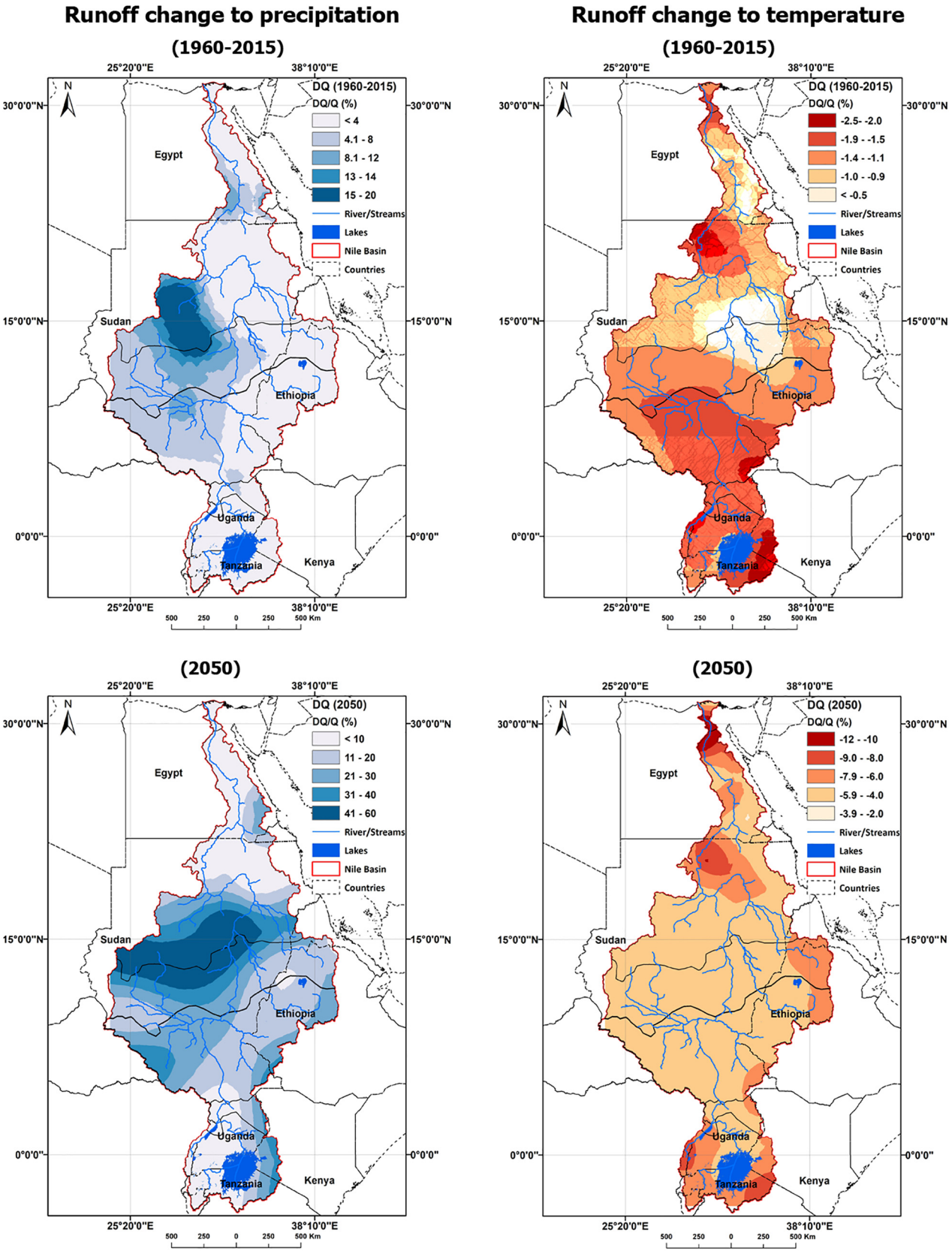

Fig. 10. Interpolated runoff elasticities (ε_p and ε_T). Areas with low ε_p values display relatively high ε_T, reflecting the inverse response of runoff to precipitation and temperature changes.

GCMs are in strong and unanimous agreement that the NRB will experience an increase in temperature of between 2 °C and 4 °C by mid-century. The same models are split, however, about the direction and magnitude of possible future precipitation change. These two processes tend to produce opposite effects on runoff; increasing precipitation implies increasing runoff while increasing temperature implies decreasing runoff. Additionally, given significant temporal and spatial variability, the trends, magnitudes and net effects of precipitation and temperature changes on runoff will likewise vary over time as well as throughout the basin.

In this paper, we utilized the Budyko Curve and the analytical forms derived by Arora (2002) to quantify changes in surface runoff due to hypothetical changes in precipitation and temperature (within the range of projections), under natural conditions. The data utilized consist of gauge-corrected precipitation, temperature, runoff, and actual and potential evaporation, as well as the projected future precipitation and temperature changes. The results show that:

1. Within the tropical zone, runoff sensitivity is about 1.6 in response to precipitation change and −0.35 in response to temperature. In other words, for comparable percentage change (e.g. 10%), precipitation exerts an impact on runoff five times the influence of temperature. Thus, in this zone, a 10% precipitation increase leads to a 16% increase in runoff while a 10% temperature increase leads to 3.5% runoff decrease. The net effect, assuming both changes occur simultaneously, will be 12.5%.
2. The magnitude of the runoff response increases with aridity. Thus, in the arid zone, runoff sensitivity is about 2.65 in response to precipitation change and −0.99 in response to temperature change. Given 10% change in precipitation, therefore, runoff will increase by 26.5%. In contrast, a 10% temperature change will reduce runoff by nearly 10%. The effect of both events occurring simultaneously is a net 16.5% increase in runoff.
3. Runoff response to precipitation change is strongly non-linear across the basin. That is, the increase in runoff due to a 10% precipitation increase is significantly different from the decrease in runoff due to a 10% runoff decrease. On the other hand, runoff response to temperature change may be considered approximately linear; in general, a 10% increase in temperature produces an approximately proportional change in runoff as a 10% temperature decrease.
4. The elasticity of runoff to precipitation and temperature is not time-invariant. Over time, it is likely to change either as a result of natural or human activities or more likely the combination of both, necessitating periodic updates of the *Q-P-T* relationships and the ensuing elasticity.
5. While developed based on changes in the mean, the method can readily be extended to investigate the effects of extreme variability, by calculating the runoff response to extreme events during the observational period.
6. As applied in this paper, the effects of human activities on runoff response are only implicitly captured. Because human actions and decisions account increasingly for the larger proportion of basin-scale changes, future research is needed to account explicitly for the effects of human agency in this method.
7. This research demonstrates the value of global gauge-corrected grids for understanding the hydrology of complex basins, such as the Nile Basin, where access to *in situ* data is limited.

In sum, the paper showed that the elasticity approach is a robust, fast and intuitive method for estimating runoff changes using a limited set of hydroclimatic variables. In data scarce regions, therefore, the method can be applied to produce results with accuracy sufficient for many practical applications.

Acknowledgements

The authors thank the Institute for Study of Human Flourishing (ISHF) at the University of Oklahoma (OU), United States, for providing research funds for this study to the first author in form of a Ph.D. dissertation fellowship. Thanks also go to the Advanced Radar Research Center and the Hydrometeorology and Remote Sensing Laboratory at OU for providing the research facilities, workspace, and equipment to accomplish this research. We are grateful to the two anonymous reviewers, the editor and the associate editor for providing valuable comments and directions on our manuscript.

We also thank the providers of important remote sensing and reanalysis datasets used in this research: the NASA Goddard Earth Science Data and Information Service Centers, the Climatic Research Unit at the University of East Anglia, the National Oceanic and Atmospheric Administration, the Global Precipitation Climatological Center, and the Global Runoff Data Centre.

References

Abtew, W., Melesse, A.M., 2014. The Nile River Basin. Nile River Basin 7–21.
Arora, V.K., 2002. The use of the aridity index to assess climate change effect on annual runoff. J. Hydrol. 265, 164–177.
Beyene, T., Lettenmaier, D.P., Kabat, P., 2009. Hydrologic impacts of climate change on the Nile River Basin: implications of the 2007 IPCC scenarios. Clim. Change 100 (3–4), 433–461.
Camberlin, P., 2009. Nile Basin climates. In: Dumont, H.J. (Ed.), The Nile: Origin, Environments, Limnology and Human Use. Springer, Monographiae Biologicae, pp. 307–333.
Chiew, F.H.S., 2006. Estimation of rainfall elasticity of streamflow in Australia. Hydrol. Sci. J. 51 (4), 613–625.
Chiew, F.H.S., Peel, Murray C., Mcmahon, T.A., Siriwardena, L.W., 2006. Precipitation elasticity of streamflow in catchments across the world. In: Climate Variability and Change—Hydrological Impacts (Proceedings of the Fifth FRIEND World Conference). IAHS Publ, Havana, pp. 308.
Conway, D., 2005. From headwater tributaries to international river: observing and adapting to climate variability and change in the Nile basin. Global Environ. Change 15 (2), 99–114.
Conway, D., Hulme, M., 1996. The impacts of climate variability and future climate change in the Nile Basin on water resources in Egypt. Int. J. Water Resour. Dev. 12 (3), 277–296.
Creed, I.F., Spargo, A.T., Jones, J.A., Buttle, J.M., Adams, M.B., Beall, F.D., Booth, E.G., Campbell, J.L., Clow, D., Elder, K., Green, M.B., Grimm, N.B., Miniat, C., Ramlal, P., Saha, A., Sebestyen, S., Spittlehouse, D., Sterling, S., Williams, M.W., Winkler, R., Yao, H., 2014. Changing forest water yields in response to climate warming: results from long-term experimental watershed sites across North America. Global Change Biol. 20 (10), 3191–3208.
Dessie, M., Verhoest, N.E.C., Pauwels, V.R.N., Admasu, T., Poesen, J., Adgo, E., Deckers, J., Nyssen, J., 2014. Analyzing runoff processes through conceptual hydrological modeling in the Upper Blue Nile Basin, Ethiopia. Hydrol. Earth Syst. Sci. 18 (12), 5149–5167.
Di Baldassarre, G., Elshamy, M., van Griensven, A., Soliman, E., Kigobe, M., Ndomba, P., Mutemi, J., Mutua, F., Moges, S., Xuan, Y., Solomatine, D., Uhlenbrook, S., 2011. Future hydrology and climate in the River Nile basin: a review. Hydrol. Sci. J. 56 (2), 199–211.
Dile, Y.T., Berndtsson, R., Setegn, S.G., 2013. Hydrological response to climate change for Gilgel Abay River, in the Lake Tana Basin – Upper Blue Nile Basin of Ethiopia. PLoS One 8 (10), e79296.
Dooge, J.C.I., Bruen, M., Parmentier, B., 1999. A simple model for estimating the sensitivity of runo to long-term changes in precipitation without a change in vegetation. Adv. Water Resour. 23, 153–163.
Elshamy, M.E., Baligira, R., Abdel-Ghaffar, E., Moges, S.A., 2009a. Investigating the climate sensitivity of different Nile Sub-Basins. In: Thirteenth International Water Technology Conference, IWTC 13 Hurghada, Egypt, pp. 17–31.
Elshamy, M.E., Seierstad, I.A., Sorteberg, A., 2009b. Impacts of climate change on Blue Nile flows using bias-corrected GCM scenarios. Hydrol. Earth Syst. Sci. 13 (5), 551–565.
Fekete, B., Vörösmarty, C., Grabs, W., 2002. Global Composite Runoff Fields on Observed River Discharge and Simulated Water Balances Water System Analysis Group, University of New Hampshire, and Global Runoff Data Centre. Federal Institute of Hydrology (BfG), Koblenz, Germany.
Fick, S.E., Hijmans, R.J., 2017. Worldclim 2: new 1-km spatial resolution climate surfaces for global land areas. Int. J. Climatol.
Gebrekristos, S.T., 2015. Understanding Catchment Processes and Hydrological Modelling in The Abay/Upper Blue Nile Basin, Ethiopia. Delft University of Technology, CRC Press/Balkema, The Netherlands., pp. 167.
Gleick, P.H., 1991. The vulnerability of runoff in the Nile basin to climatic changes. Environ. Professional 13, 66–73.
Grijsen, J.G., Tarhule, A., Brown, C., Ghile, Y.B., Taner, U., Talbi-Jordan, A., Doffou, H.N., Guero, A., Dessouassi, R.Y., Kone, S., Coulibaly, B., Harshadeep, N., 2013. Climate

Risk Assessment for Water Resources Development in the Niger River Basin Part II: Runoff Elasticity and Probabilistic Analysis.
Gudmundsson, L., Wagener, T., Tallaksen, L.M., Engeland, K., 2012. Evaluation of nine large-scale hydrological models with respect to the seasonal runoff climatology in Europe. Water Resour. Res. 48 (11).
Harman, C.J., Troch, P.A., Sivapalan, M., 2011. Functional model of water balance variability at the catchment scale: 2. Elasticity of fast and slow runoff components to precipitation change in the continental United States. Water Resour. Res. 47 (2) n/a–n/a.
Hasan, E., Elshamy, M., 2011. Application of hydrological models for climate sensitivity estimation of the Atbara Sub-basin. Nile River Basin 227–240.
Hasan, E., Kirstetter, P., Zhang, K., Hong, Y., 2015. The Challenges and Opportunities of Hydrologic Remote Sensing in Data-Poor Regions: Case Study of Nile River Basin. AGU Fall Meeting Abstracts, pp. 51.
Ibrahim, A.M., 2011. The Nile Basin cooperative framework agreement: the beginning of the end of Egyptian hydro-political hegemony. Missouri Environ. Law Policy Rev. (MELPR) 18 (2).
IPCC, 2014. Climate Change 2014: Synthesis Report. Contribution of Working Groups I, II and III to the Fifth Assessment Report of the Intergovernmental Panel on Climate Change, Geneva, Switzerland.
Jones, P.D., Harris, I.C., 2013. CRU TS3.21: Climatic Research Unit (CRU) Time-Series (TS) Version 3.21 of High Resolution Gridded Data of Month-by-month Variation in Climate (Jan. 1901–Dec. 2012). University of East Anglia Climatic Research Unit, NCAS British Atmospheric Data Centre.
Labat, D., Goddéris, Y., Probst, J.L., Guyot, J.L., 2004. Evidence for global runoff increase related to climate warming. Adv. Water Resour. 27 (6), 631–642.
Martens, A.K., 2011. Impacts of Global Change on the Nile Basin Options for Hydropolitical Reform in Egypt and Ethiopia. IFPRI Discussion Paper 01052.
Mohamed, Y., Loulseged, M., 2008. The Nile Basin Water Resources: Overview of Key Research Questions Pertinent to the Nile Basin Initiative, Colombo, Sri Lanka.
NIS, 2012. Climate Change and its Implications for the Nile Region. (Chapter 8).
Oestigaard, T., 2010. Nile Issues, Small Streams from the Nile Basin Research Programme. Fountain Publishers, Kampala-Uganda.
Sankarasubramanian, A., Vogel, R.M., Limbrunner, J.F., 2001. Climate elasticity of streamflow in the United States. Water Resour. Res. 37 (6), 1771–1781.
Schaake, J.C., 1990. From climate to fow. In: Waggoner, P.E. (Ed.), Climate Change and U.S. Water Resourcese. John Wiley, New York, pp. 77–206.
Schneider, U., Becker, A., Meyer-Christoffer, A., Ziese, M., Rudolf, B., 2011. Global Precipitation Analysis Products of the GPCC, Deutscher Wetterdienst. Offenbach a.M., Germany.
Setegn, S.G., Rayner, D., Melesse, A.M., Dargahi, B., Srinivasan, R., 2011. Impact of climate change on the hydroclimatology of Lake Tana Basin, Ethiopia. Water Resour. Res. 47 (4) n/a–n/a.
Shahin, M., 1985. Hydrology of the Nile Basin. Elsevier Science Publishing Company Inc., New York.
Siam, M.S., Eltahir, E.A.B., 2017. Climate change enhances interannual variability of the Nile river flow. Nat. Clim. Change.
Swain, A., 2011. Challenges for water sharing in the Nile basin: changing geo-politics and changing climate. Hydrol. Sci. J. 56 (4), 687–702.
Taye, M.T., Ntegeka, V., Ogiramoi, N.P., Willems, P., 2011. Assessment of climate change impact on hydrological extremes in two source regions of the Nile River Basin. Hydrol. Earth Syst. Sci. 15 (1), 209–222.
UNEP, 2013. Adaptation to Climate-change Induced Water Stress in the Nile Basin: A Vulnerability Assessment Report.
van der Velde, Y., Vercauteren, N., Jaramillo, F., Dekker, S.C., Destouni, G., Lyon, S.W., 2014. Exploring hydroclimatic change disparity via the Budyko framework. Hydrol. Process. 28 (13), 4110–4118.
Williams, M.A.J., 2009. Human impact on the Nile Basin: past, present, future. In: Dargahi, B. (Ed.), The Nile: Origin, Environments, Limnology and Human Use. Springer, Monographiae Biologicae.
Yang, H., Yang, D., 2011. Derivation of climate elasticity of runoff to assess the effects of climate change on annual runoff. Water Resour. Res. 47 (7) n/a–n/a.
Zhang, K., Kimball, J.S., Nemani, R.R., Running, S.W., 2010. A continuous satellite-derived global record of land surface evapotranspiration from 1983 to 2006. Water Resour. Res. 46 (9).